ACCEPTED FOR PUBLICATION
13 February 2019
Journal of Anatomy NIHMS:
NIHMSID1012211

Cervical vertebral body growth and emergence of sexual dimorphism: A developmental study using computed tomography

Authors (First, Middle Initial, Last):

Courtney A. Miller, MSc
Associate Research Specialist, Vocal Tract Development Lab
Waisman Center, University of Wisconsin-Madison

Seong Jae Hwang, MSc
PhD Candidate
Department of Computer Sciences, University of Wisconsin-Madison

Meghan M. Cotter, Ph.D.
Lecturer, Gross Anatomy Teaching Group
Academic Affairs, University of Wisconsin School of Medicine and Public Health

and

Houri K. Vorperian, Ph.D.
Senior Scientist, Vocal Tract Development Lab
Waisman Center, University of Wisconsin-Madison

Corresponding Author:

Houri K. Vorperian, Ph.D.
1500 Highland Avenue, Rm 427
Madison, WI 53705
Telephone: (608) 263-5513
Fax: (608) 263-5610
E-mail: vorperian@waisman.wisc.edu

Abstract

The size and shape of human cervical vertebral bodies serve as a reference for measurement or treatment planning in multiple disciplines. It is therefore necessary to understand thoroughly the developmental changes in the cervical vertebrae in relation to the changing biomechanical demands on the neck during the first two decades of life. To delineate sex-specific changes in human cervical vertebral bodies, 23 landmarks were placed in the midsagittal plane to define the boundaries of C2 to C7 in 123 (73 M; 50 F) computed tomography scans from individuals, ages 6 months to 19 years. Size was calculated as the geometric area, from which sex-specific growth trend, rate, and type for each vertebral body were determined; as well as length measures of local deformation-based morphometry vectors from the centroid to each landmark. Additionally, for each of the four pubertal-staged age cohorts, sex-specific vertebral body wireframes were superimposed using generalized Procrustes analysis to determine sex-specific changes in form (size and shape) and shape alone. Our findings reveal that C2 was unique in achieving more of its adult size by five years, particularly in females. In contrast, C3-C7 had a second period of accelerated growth during puberty. The vertebrae of males and females were significantly different in size, particularly after puberty, when males had larger cervical vertebral bodies. Male growth outpaced female growth around age 10 years and persisted until around ages 19-20 years where as females completed growth earlier, around ages 17-18 years. The greatest shape differences between males and females occurred during puberty. Both sexes had similar growth in the superoinferior height, but males also displayed more growth in anteroposterior depth. Such prominent sex differences in size, shape, and form are likely the result of differences in growth rate and growth duration. Female vertebrae are thus not simply smaller versions of the male vertebrae. Additional research is needed to further quantify growth and help improve age- and sex-specific guidance in clinical practice.

Keywords: cervical vertebrae, vertebral body, growth and development, sexual dimorphism, size and shape, Cervical Vertebral Maturation Index, computed tomography, human.

Introduction

During human development, cervical vertebral bodies undergo changes in size and shape before reaching their adult morphology (Huelke, 1998, Kumaresan et al., 2000). The ontogeny of cervical vertebral bodies (C2-C7) occurs through of primary and secondary ossification centers. The C2 vertebral body forms from three primary ossification centers and one apical secondary ossification center, while C3-C7 vertebral bodies each form from one primary ossification center and two secondary ossification centers (Akobo et al., 2015, Byrd and Comiskey, 2007, Piatt and Grissom, 2011, Yoganandan et al., 2011). These patterns of ossification and resulting development in size and shape of cervical vertebrae support the primary functions to protect the spinal cord and nerves and to enable mobility and support of the head and neck. Cervical vertebral bodies undergo endochondral ossification and develop morphology that increases contact between the vertebrae, supporting the shift from greater mobility of the neck in children to greater stability in adults (Huelke, 1998, Kumaresan et al., 2000). Furthermore, human bipedal locomotion shifts the line of gravity along the vertebral column, forming cervical lordosis which, in combination with changes in the head-to-body ratio, changes the fulcrum of cervical movement (primarily flexion/extension) from C2-C3 in infancy, to C4-C5 by around age 5 years, and to C5-C6 (the adult location) by late adolescence (Huelke, 1998, Lustrin et al., 2003, Kokoska et al., 2001).

Various disciplines use the cervical vertebral bodies as a reference for describing developmental changes of adjacent structures. For example, speech scientists and evolutionary biologists use the vertebral level as a reference to assess the descent of the larynx to understand the development of the vocal tract and the evolution of human speech (Boë et al., 2006, Lieberman, 2007, Bench, 1963, Lieberman et al., 2001). Developmental changes of the cervical vertebral bodies can be used to identify the biological age of a patient or for clinical decision-making, such as the clinical diagnosis of pediatric trauma (Nitecki and Moir, 1994, Gilsanz et al., 1997, Kokoska et al., 2001), or identifying the level of proper velopharyngeal closure correction in patients with cleft palate (Mason et al., 2016). Similarly, orthodontists use cervical vertebral body morphological stages to identify the biological age of a patient to determine appropriate treatment (Altan et al., 2011, Bench, 1963). Sex differences in growth have been determined (Been et al., 2017, Ezra et al., 2017), yet most clinical standards of cervical vertebral assessment continue to use unisex standards.

Since the 1970s, cervical spine research has advanced from descriptive and visual assessment of cadavers, archaeological remains, and lateral cephalometric images (Bick and Copel, 1950, Francis, 1955, Tulsi, 1971) to establish the Cervical Vertebral Maturation Index (CVMI) for identifying maturation stages based on visual assessment of cervical vertebra shape, (Hassel and Farman, 1995, Pichai et al., 2014, San Román et al., 2002, Byrd and Comiskey, 2007, Nestman et al., 2011, Santiago et al., 2012, Yang et al., 2014). Briefly, CVMI determines six stages of skeletal maturation based on visual assessment of morphological changes characteristic of cervical spine development in relation to mandibular growth (Hassel and Farman, 1995, Jaqueira et al., 2010, San Román et al., 2002). The stages are typically associated with an age range of 8 years to 17 years, ages surrounding the pubertal growth spurt (PGS) (Carinhena et al., 2014, Santiago et al., 2012). While CVMI is commonly used by orthodontists to identify biological age, some researchers question its value in assessing skeletal maturity due to the poor reliability between researchers in visually classifying shape to the same CVMI stage (Gray et al., 2016, Johnson et al., 2016, Nestman et al., 2011, Santiago et al., 2012, Yang et al., 2014); poor improvement over use of chronological age (Chatzigianni and Halazonetis, 2009); and not accounting for sexual dimorphism of the cervical spine (Caldas et al., 2007).

With advances in medical imaging and related computational programs, researchers have begun to quantify the growth of the cervical spine in size and morphology. Examples include researchers quantifying CVMI using linear measurements of the cervical spine (dos Santos et al., 2010, Altan et al., 2011) or by digitizing the morphological changes during development and identifying discrepancies between CVMI and the relational mandibular growth peak (Gray et al., 2016). Additional examples include: quantifying linear and angular measures on CT scans to assess the development of select cervical vertebral features (Kasai et al., 1996, Altan et al., 2011) or the morphological changes of the craniovertebral junction (Piatt and Grissom, 2011); quantifying the growth of all cervical vertebral bodies during the first 18 years by calculating linear measures in the mid-sagittal plane (Johnson et al., 2016, Wang et al., 2001); and quantifying the emergence of sexual dimorphism by using landmark-based measurements to assess vertebral body geometry (Hellsing, 1991). Such quantitative analyses contribute to our understanding of developmental trends of growth in size and shape of cervical vertebrae.

Nonlinear growth trends have been documented since Scammon (1930) classified four primary growth types for different structures/organs with each growth type having its unique growth curve/trend. However, Scammon (1930) highlighted that the neck and some head structures exhibit a combination of two growth types, general and neural. The general growth type, as described by Scammon (1930), exhibits two distinct periods of accelerated growth, the first occurring from birth to the age of 5 or 6 years where about a quarter of the adult size is attained, and the second period of accelerated growth occurring during puberty where sexual dimorphism typically becomes most evident and where females reach the adult mature size sooner than males (Scammon, 1930, Hellsing, 1991). This general growth type is also referred to as skeletal growth, or somatic growth – term used in this paper – because it generally applies to structures of mesodermal (somite) tissue. The neural growth type, on the other hand, exhibits accelerated growth during the first 5-6 years of life, where two-thirds of the adult size is attained and is followed by steady growth until the adult size is reached (Nellhaus, 1968, Scammon, 1930). The neural growth type is typically associated with a combination embryological origin of ectoderm, mesoderm, and neural crest tissue, which develops into the brain and cranium.

The primary purpose of this study was to analyze the sex-specific growth and development of the cervical vertebral bodies C2-C7, in size and shape in the midsagittal plane, and to assess when sexual dimorphism emerges. Considering the form-function relationship, and given that all cervical vertebral bodies are formed from the same embryological origin tissue (sclerotome of somites), have serially homologous structure, and the same function of flexion-extension, we expected that the C2-C7 vertebral bodies would have similar nonlinear growth trends. We hypothesized that all cervical vertebral bodies would follow a predominantly somatic growth type, but anticipated C2 growth to be slightly different, given the additional functional demand of rotation with C1 and morphological variation. In addition, we hypothesized that the vertebral bodies would show sexual dimorphism –in size but not necessarily shape- consistent with the sex-specific growth standards developed by the Centers for Disease Control and Prevention (CDC) and World Health Organization (WHO) for head circumference, stature and weight.

Material and Methods

Material: Medical imaging studies and image acquisition

A retrospective developmental head and neck imaging database was used to select the dataset for this study. The database was established by the Vocal Tract Development Lab (VTLab) at the Waisman Center, with approval from the University of Wisconsin Health Sciences Institutional Review Board, for the purpose of studying the growth of vocal tract structures in the oral and pharyngeal regions. The VTLab database consists of imaging studies from individuals across the lifespan who were imaged one or more times, at the University of Wisconsin Hospital and Clinics, for various medical reasons unrelated to skeletal growth and development, such as evaluations of abscesses, neck masses, or trauma. All scans were acquired with patients in the supine body position with their head oriented centrally in the scanner utilizing the laser light guidance of the scanner. The scans, saved in Digital Imaging and Communications in Medicine (DICOM) format, were alphanumerically coded and included in the VTLab database. Our radiologist collaborators, with expertise in the head and neck, verified medical diagnosis from medical records and confirmed each scan met the inclusion criteria for this developmental imaging database, such as no history or evidence of medical conditions that could disrupt typical growth and development of the head and neck. For additional information on medical imaging acquisition parameters and inclusion criteria, refer to (Vorperian et al., 2009). Based on the National Center of Health Statistics growth charts for boys and girls (CDC, 2000), the majority of reported weights at time of scan were at the 50th percentile with all scans between the 25th and 95th percentile (Vorperian et al., 2009).

The dataset selected from the VTLab imaging database for this study consisted of 123 computed tomography (CT) scans (50 females and 73 males) from 6 months to 20 years of age.

Imaging studies were acquired using the General Electric helical CT scanner using the following parameters:14.0-22.0 cm field of view, 512 x 512 matrix, 100-130 kV, 46-360 mA, and slice thickness of less than 3.75 mm, with the majority being 2.5 mm (n=87) and 1.25 mm (n=26). Additionally, the in-plane resolution/voxel size of the imaging scans in this study ranged from 0.2051 mm to 0.5859 mm with a majority at 0.3516 mm (n=41) or 0.3125 mm (n=25). Several GE reconstruction algorithms were applied to the raw CT image data to optimize visualization of soft tissue (standard, soft) and bony (bone) structures. This study included predominately Standard algorithm scans (n=110). Bone (n=5) and soft (n=8) algorithms were included to effectively increase the age and sex specific sample size when the Standard algorithm was not available. All CT scans were visually inspected and excluded from this study if there was movement detected in the CT scan, if the whole cervical spine was not visible, or if atypical development was suspected.

Landmarking cervical vertebral bodies

To quantify the growth in the cervical spine, 23 anatomic landmarks were placed on each scan defining the anatomical boundary of the C2-C7 vertebral bodies in the midsagittal plane (see Figure 1, left panel). C1 was excluded from analysis due to the lack of a weight-bearing vertebral body. Three researchers placed the landmarks on all 123 cases, with duplicate landmarks placed on a subset of five cases to assess both landmark placement and landmark-based measurement reliability. Landmark placement entailed placing three landmarks on C2, and four on each of C3-C7 using the Fabricate tool in the Analyze 12.0® software package (AnalyzeDirect, Overland Park, KS) utilizing multiple viewing planes (sagittal, coronal, and axial) of the original DICOM images to guide the placement of each landmark's x, y, and z coordinates. Connecting the landmarks created a wireframe shape of each cervical vertebral body, hereafter called a vertebral wireframe. All landmark coordinates were scaled to millimeters (mm) based on the voxel size of the respective CT scan.

Pre-process step: 3D landmarks to 2D plane

Prior to geometric area and local deformation-based morphometry (LDBM) calculation and analysis, all 123 CT studies were pre-processed to compensate for potential deviations in head position and ensure each vertebral wireframe was in the true anatomical midsagittal plane. The pre-process entailed two steps to convert the 3D (x, y, z) landmark coordinates, which might not be coplanar, into a 2D (y,z) midsagittal vertebral wireframe. First, using the landmarks of each individual vertebral wireframe, the best-fit midsagittal plane was computed in a least squares manner and the landmarks were projected onto that plane while maintaining their relationship with the centroid. This ensured the wireframe landmarks were on a perfect 2D midsagittal plane. Next, the corrected midsagittal plane and landmarks were rotated to a common x-axis plane, removing the third (x) dimension. The landmarks were then connected to create the 2D vertebral wireframe to calculate size, using geometric area, and assess changes in shape and form (i.e., shape with size) as further defined in the "Cervical vertebral body measurements: Size and form" section and the "Morphology: Growth in shape and form" section respectively. This pre-process 3D to 2D step reduced the distance by an average 0.25mm in landmark placement between raters, increasing reliability. Both raw and aligned landmark coordinates are provided in Supplemental Tables I and II.

Cervical vertebral body measurements: Size and form

Once the 2D wireframes were identified, sex-specific developmental changes in size and form were quantified as follows: first, the geometric area (mm^2), employing the 2D polygon area formula, was calculated as a global measure in size of each vertebral wireframe using the anterior-posterior (y) and superior-inferior (z) coordinates of each landmark. Next, the Euclidian distance from the centroid to each individual landmark was calculated to quantify the change in the form of each vertebral wireframe. These LDBM measures were used to define the displacement vector of each landmark from the centroid (geometric center) of each vertebral wireframe, allowing examination of the changes in the relative positions of each landmark and identification of the localized changes in vertebral body form during growth (Ashburner and Friston, 2000). The C2 vertebral wireframes consisted of three LDBM vectors, while C3-C7 each consisted of four LDBM vectors. To assess measurement reliability between raters, inter class correlation (ICC) was calculated. ICC for geometric area was > 0.94, and for LDBM was > 0.89, implying strong reliability in reproducibility of both geometric area and Euclidean distance LDBM calculations.

Analysis

Geometric Area: Growth in size

Based on the understanding that human growth and development is non-linear, the geometric area results for each cervical vertebral body were calculated using the pre-processed 2D vertebral wireframe landmarks and plotted as a function of age along with a fourth degree polynomial fit. In line with previous research characterizing the growth of oral/pharyngeal structures (Vorperian et al., 2009), this model fit optimally characterized the growth of geometric areas despite the limitation of the polynomial fit at the extreme ages. The five female (F) cases and three male (M) cases that had measurements for one vertebral body over 2.567 standard deviations away from the fit were identified as outliers (Wang et al., 2013) and excluded from all analyses. The data from the remaining 115 cases (45 females and 70 males) were refitted with the fourth degree polynomial fit and plotted with a second y-axis for percent of adult growth, an important reference to have when assessing for growth type (neural or somatic; Figure 1, middle panel). In addition, the first derivative of this polynomial fit was plotted (Figure 1, right panel) to examine growth rate. To quantitatively determine growth type (neural versus somatic), a composite growth model comprised of a linear combination of a neural and somatic growth types (Wang et al., 2013) was applied to the geometric areas to calculate the percent contribution of somatic and neural growth types towards the overall geometric area growth trends.

Finally, to assess sex differences, an ANOVA test was conducted to identify if there were overall significant male versus female differences in fourth degree polynomial model fits for growth in size/area. However, given growth rate differences, and to better determine when sexual dimorphism emerges, additional localized analysis of sex differences was performed, using either a t-test or the Mann-Whitney test, between the following four pubertal-specific age cohorts: cohort I (pre-pubertal) ages birth to 4:11 years (4 years and 11 months, n=47, 10F, 37M); cohort II (peri-pubertal) ages 5 years to 9:11 years (n=20, 10F, 10M); cohort III (puberty) ages 10 years to 14:11 years (n=20, 10F, 10M); and cohort IV (post-pubertal) ages 15 years to 19:11 years (n= 28, 15F, 13M).

LDBM: Growth in size and form

The LDBM measures, described above in the "Cervical vertebral body measurements: Size and form" section, provide a landmark-specific approach to quantify where and when the changes in size and shape occur for males and females. The LDBM averages and standard deviations were calculated for each sex-specific cohort. Next, for each age cohort, a t-test or Mann-Whitney U test was conducted to assess sexual dimorphism of the LDBM at each landmark. Given the multiple comparisons, the Bonferroni correction was applied to eliminate alpha one error (Bland and Altman, 1995).

Morphology: Growth in shape and form

While the geometric areas provide information on the sex-specific global size growth trend, rate, and type for each cervical vertebral body, examination of growth in relation to morphological change provides visualization of the sex differences and localized variation in shape based on change at each landmark. ‘Shape’ is defined as the geometric information remaining after removing size, position, and orientation, while ‘form’ is the geometric information when maintaining size and removing position and orientation (Dryden and Mardia, 2016). Given the discourse on whether there is covariance between size and shape (Klingenberg, 2016), this study visualized both the shape and the form of the cervical vertebral bodies. Once the 2D vertebral wireframes were determined in the pre-processing step, the cases were superimposed using generalized Procrustes analysis (GPA), hereafter referred to as full GPA. The full GPA allows assessment of shape alone by removing the orientation, position, and scale of each vertebra to optimally align all wireframes (Zelditch et al., 2004). The cases were also superimposed using partial GPA, which removes orientation and position but maintains the size of each vertebra, allowing the assessment of form (Zelditch et al., 2004). By not scaling, it is possible to maintain the magnitude of growth at each landmark and visualize the average form variance during development. Both full and partial GPA were applied to each age cohort per sex using, respectively, *gpagen* function from the ‘geomorph’ R package (Adams et al., 2013) and *ProcGPA* function from the ‘shapes’ R package (Claude, 2008, Dryden and Mardia, 2016). Given the developmental nature of this study, the vertebrae were grouped by age cohort per sex to minimize the impact of sex and size when applying the full and partial GPA (Mitteroecker et al., 2013) and to identify the best sex-specific mean shapes and forms for each age cohort. The assessment of sexual dimorphism of shape for each age cohort was conducted by superimposing the male and female full GPA mean shapes for each age cohort (Figure 3). The sex-specific age cohort partial GPA mean forms were superimposed to visualize the age-specific changes in females (Figure 4, left panel) and males (Figure 4, right panel) as well as to identify the average growth trajectories at each landmark for males and females (Figure 4, central panel).

Results

Geometric Area: Growth trend and growth rate

In general, for both males and females, all vertebral bodies (C2-C7) exhibited growth in size/area with an accelerated growth period during the first five years of life. Growth trend graphs (Figure 1, center panel) present sex-specific data, each with a fourth degree polynomial fit. These growth trend graphs also show the percent growth of adult size as displayed on the second y-axis. The mature male and female size is identified at 100% when the growth trend reaches the maximum size. The negative growth fit evident for C3-C7, particularly after age 17 years, reflects a minor boundary limitation of the curve-fitting technique due to limited data at the later ages (De Boor, 1978). Examination of the growth trends/trajectories reveal that C2 has a different growth trend than C3-C7 in that C2 growth attains more adult size at a younger age than C3-C7. In addition, C3-C7 growth rate graphs (Figure 1, right panel) show an increase in growth rate for both males and females at about age 6 to 10 years with male growth rates outpacing females at about age 10 years, which results in a second accelerated growth period during the pubertal ages 12 years and onward as evident in the growth trends. Although C2 similarly displays an increase in growth rate in males at about 10 to 12 years, the increase in rate is smaller compared to C3-C7.

Geometric Area: Neural and/or somatic growth type

To quantify the growth type (neural versus somatic) of each of the cervical vertebral body, we applied a composite growth model to the geometric growth areas (Wang et al., 2013). Findings of the percent of similarity to neural and somatic growth types for each cervical vertebra are summarized in Table 1. The results reveal that most of the cervical vertebrae, specifically C3-C7, had somatic growth type in males and females, which is in line with what we had hypothesized and also observed in the area growth trend findings described above. However, the finding that C2 has a predominantly neural growth type in females (96.2%) and a combination of neural/somatic in males (59.2% / 40.8%) was unexpected, though not surprising given its proximity and attachment to the skull as well as the additional functional demand of head rotation unique to the C2 vertebra.

Geometric Area: Sexual dimorphism

Sexual dimorphism of the sex-specific growth trends for geometric area was significant for all vertebrae at the Bonferroni corrected $\alpha = 0.05$ significance level of 0.008. By the age of maturity female cervical vertebral bodies were smaller than male cervical vertebral bodies, these differences were not present throughout development (Figure 2). On the contrary, by age 5 years, females attain on average 7% more of their adult vertebral sizes than males (Figure 1, center panel). Furthermore, the growth trends show that female vertebrae were larger than male vertebrae for C2, until 12 years, for C3-C5, until 13 years, and for C6-C7 until 15 years. As seen in the growth rate graphs (Figure 1, right panel) at around 10 years all male cervical vertebral bodies show more growth per month than females, and male vertebral bodies become larger than females between the ages of 12 to 15 years. Additionally, females reached adult size for C3-C7 at 17-18 years, while males continued to grow until about 19-20 years (Figure 1).

To determine when sexual dimorphism emerges, localized age analyses were carried out using the four age cohorts described in the methods section, with the Bonferroni corrected $\alpha = 0.05$ significance level of 0.002. Findings revealed sexual dimorphism to be present only after puberty (i.e., during age cohort IV) for all vertebrae (Figure 2). During the pre-pubertal (age cohort I) and pubertal (age cohort III) stages, the female mean and median geometric areas were larger than those of males, however such differences were not significant. During the peri-pubertal (age cohort II) stage, the mean and median geometric areas were nearly equivalent. During the post-pubertal (age cohort IV) stage, sexual dimorphism emerged with male geometric areas being significantly larger than those of females in all vertebrae.

LDBM: Size and form

The LDBM sex-specific averages for each age cohort and standard deviation (see Supplemental Tables III-IV) support the geometric area findings that males grew more than females at all landmarks. The p-values from the t-test/Mann-Whitney U test for sexual dimorphism in each age cohort are presented in Table 2 for LDBM, with the Bonferroni corrected $\alpha = 0.05$ significance level of 0.0125. All landmarks presented significant sex differences in LDBM during cohort IV with the exception of C2 apex, C6 posterior-superior, and C2, C3, and C7 anterior-inferior.

Morphology: Shape and form

The mean wireframe shapes from the full GPA are presented in Figure 3, while the mean wireframe forms and growth trajectories from the partial GPA are presented in Figure 4. The mean vertebral wireframe shapes for each age cohort for males and females support the morphological changes associated with the CVMI stages: horizontal rectangle to wedge shape to square to vertical rectangle. These stages were more evident in the shape changes of the male vertebral bodies. As seen in Figure 3, the female shapes were similar in cohorts III and IV, suggesting females obtained mature shape during cohort III. In addition, the greatest sexual dimorphism in shape was visible during cohort III. In Figure 4, the mean form wireframes for females (left panel) and males (right panel) highlight the average changes in size and shape between age cohorts in each vertebral body and permit comparison of the sex differences in size and shape during the post-pubertal stage of development (age cohort IV). To showcase sexual dimorphism in form, Figure 4 (center panel) is a proportional schematic displaying the growth vectors at each landmark from the average wireframe at age cohort I to the mean II, III, and IV male and female landmarks based on the partial GPA. Figures 3 and 4 show that the female cervical vertebral body shape had greater vertical height during all age cohorts, while males had greater horizontal depth.

Discussion

This study provides quantitative analyses of cervical vertebral bodies C2-C7 growth in size and shape throughout the first two decades of life for CT scans from 70 males and 45 females using 3D landmarks to calculate geometric area and LDBM. All cervical vertebrae displayed non-linear, non-uniform growth in size and shape. We identified two growth spurts in C3-C7, typical of a somatic growth type, while C2 had a distinct growth trend and rate, with a combined neural/somatic growth type for males and pure neural growth type for females. Sexual dimorphism was found in both the growth in size and change in shape of cervical vertebral bodies, where differences became most evident in the post-pubertal stage (cohort IV). Such prominent differences in size and shape are likely due to males outpacing female growth rate beginning at about 10 years, with sustained growth for a longer period in males, while females appear to have completed growth by about age 17 years. Such developmental as well as sex differences in size and shape of the cervical vertebral bodies likely relates to morphological sex differences of other anatomical structures in the vicinity, such as the pharynx, larynx, and speech/masticatory systems.

Growth in Size: Geometric area growth trends, rates, and types

The first five years is a biomechanically important developmental stage, when children gain control of head movement (Huelke, 1998, Kumaresan et al., 2000), the line of gravity shifts (Bogduk and Mercer, 2000, Le Huec et al., 2011), and nuchal musculature develops (Nalley and Grider-Potter, 2015) with the transition to bipedal movement. The interrelationship between growth and the biomechanical developmental stages are reflected in the rapid growth of the cervical vertebral bodies in the non-linear growth trends of this study during the first five years of life where, as seen in Figure 1, when the cervical vertebral bodies of C2 attained over 50% and C3-C7 attained about 35% of its adult size.

A second rapid growth period occurred during the pubertal growth spurt for all vertebrae, with the exception of female C2 and on a smaller scale for male C2. This rapid pubertal growth period has been associated with the CVMI stages (Carinhena et al., 2014, Shapland and Lewis, 2014). During the pubertal growth spurt, vertebral bodies of males became significantly larger than those of females (Figure 2), in agreement with previous studies (Caldas et al., 2007, Parenteau et al., 2014, Stemper et al., 2008, Yoganandan et al., 2017). Within a clinical context, the cervical vertebrae are considered to have achieved adult morphology by ages 8-10, as determined by lateral radiographs and similarity in trauma patterns for individuals over 9 years (Gilsanz et al., 1997, Menezes and Traynelis, 2008, Nitecki and Moir, 1994, Kokoska et al., 2001). However, the present study showed continued growth in age cohort IV (15-20 years), supporting the findings that growth in size continues well after 9 years (Johnson et al., 2016).

Scammon (1930) noted that the neck circumference has a complex postnatal growth pattern, following a combination of somatic and neural growth types. The distinctive growth of C2 found in this study may reflect differences in function, structure, and developmental origin. The C2 vertebral body stabilizes C1 during rotation and has increased interaction with the cranium by direct structural connection of the apical and alar ligaments from the odontoid of C2 to the cranium. The ossification pattern of C2 is distinct from that of C3-C7 due to the odontoid process, which fuses with the body of C2 between 3 and 6 years (Akobo et al., 2015). Recent research has identified a complex developmental origin of C2; while the majority of C2 develops from the sclerotome of somites, similar to all the other vertebral bodies, the apical secondary ossification center of the odontoid develops from the 4th occipital sclerotome (proatlas), which contributes to the base of the occipital bone (basioccipital) of the cranium (Akobo et al., 2015, Louryan et al., 2011, Pang and Thompson, 2011). This dual contribution in the formation of C2 explains in part why C2 has a different growth pattern from C3-C7. The developmental origin of the ossification centers and the structural connection to help with the stabilizing functional role of C2 supports a form-function interaction that may explain the predominantly neural growth type of C2 found in this study (Table 1) and likely relates to the finding that oro-pharyngeal measures follow hybrid neural/somatic growth type (Vorperian et al., 2009). However, further research into the sex differences in biomechanical development of the cervical vertebral column could provide insight as to why the contributions in growth types are different between males and females.

Growth in Shape and Form: LDBM and Morphology

While size provides a foundation for understanding growth, morphological development of cervical vertebral bodies show non-uniform changes in shape similar to the described stages in

CVMI. The mean C2–C7 shapes identified with full GPA (Figure 3) present morphological changes from a horizontal rectangle toward a slight wedge shape to a vertical rectangle shape similar to the CVMI stages (Hassel and Farman, 1995, Pichai et al., 2014, San Román et al., 2002, Byrd and Comiskey, 2007, Nestman et al., 2011, Santiago et al., 2012, Yang et al., 2014). If vertebrae in children were simply a scaled version of adult vertebrae, the vertebrae could not maintain the same biomechanical developmental pattern from greater mobility to greater stability and control of movement (Kumaresan et al., 2000, Bogduk and Mercer, 2000). Figure 3 shows that anteroposterior depth is greater before puberty in cohort I and II, suggesting greater stabilization for neck kinematics and adaption to bipedal locomotion (Figure 3). Comparative osteological analysis with other hominoids and primates suggests that the short length and wider base of the vertebral bodies in humans relates to bipedalism and less pronograde head-neck positioning (Aiello and Dean, 1990).

Humans develop cervical lordosis, allowing greater range of motion than other primates (Arlegi et al., 2017), yet the curvature is relatively less than in some quadrupedal animals due to the development of a vertical resting head and neck position (Nalley and Grider-Potter, 2015). Additionally, the degree of cervical lordosis has been attributed to the relationship between the lordotic intervertebral discs, which compensates for the kyphotic cervical vertebral body wedging. The wedging is most pronounced at age 9 months and then reduces during development as the neck becomes more stable and the child shifts to bipedal mobility (Been et al., 2017). Figures 3 and 4 support the transition to less kyphotic body wedging, which would reduce the cervical lordosis. Such findings warrant additional analysis of the vertical (superioinferior) and horizontal (anteroposterior) relational growth of the cervical vertebral bodies, which could enhance our understanding of the morphological changes found in this study.

Sexual Dimorphism

The geometric area findings of this study (Figure 1) provide sex-specific normative growth trends and rates in agreement with other studies showing that adult male cervical vertebrae are larger than adult female cervical vertebrae and that growth onset and maturation of female cervical bodies is earlier than that of males (Ezra et al., 2017, Chatzigianni and Halazonetis, 2009, Dancey et al., 2003, Yoganandan et al., 2017). While the negative growth trends for C3-C7 during cohort IV (Figure 1, center panel) could represent a reduction in size, it is more likely that it is an artifact due to a boundary limitation of the curve-fitting technique used where the fit is easily affected by the fewer number of measurements past age 17 (De Boor, 1978). Therefore, in this study we relate adult size to when the growth rate reached zero (Figure 1, right panel). Based on this interpretation, the female C3 to C7 attained adult size around 17 years, while male C2-C7 and female C2 continued to grow (Figure 1). While there was no statistical significance between the sexes in geometric area or LDBM during cohorts I to III, growth in males outpaced females at about age 10 (Figure 1, center and right panels). Further, males reached adult size at a later chronological age and at a larger size than females for all cervical vertebral bodies (Figure 1), supporting the findings that males are larger at all maturation stages (Chatzigianni and Halazonetis, 2009).

Hellsing (1991) found that the cervical vertebrae of females were larger than those of males at age 15, yet the present study of growth trend and rate has found that males became larger than females between 12 and 15 years and sexual dimorphism became significant in age cohort IV, i.e., after 15 years of age (Figure 1 and 2). Furthermore, the superior endplates during development have been known to form around puberty with complete ossification by age 18 to 25 years (Byrd and Comiskey, 2007). The finding that geometric area (Figure 2) and LDBM (Table 2) only identified significant sex differences during post-puberty, cohort IV, could suggest variance in male and female thickness of the superior endplate.

In addition to sexual dimorphism in size, the morphological results of this study reveal that male cervical vertebral bodies are not simply larger forms of female vertebrae. Female shapes had slightly more vertical (superioinferior) height while males had more horizontal (anteroposterior) depth in most age cohorts, especially during pubertal and post-pubertal stages, age cohorts III – IV (Figures 3 and 4), supporting previous findings that males and females have variance in the internal structure of cervical lordosis (Been et al., 2017). The distinct differences in cervical vertebral body form between the adult male and female vertebral bodies could provide clinicians with greater understanding of pathology and treatment (Caldas et al., 2007, Dancey et al., 2003, Mason et al., 2016, Yoganandan et al., 2017). The differences in size and shape have been theorized as a cause for decreased spinal stability in females and could also be a contributing factor to the disparity in male and female range of motion (Seacrist et al., 2012), but further research is needed. The biomechanical stability variance between males and females has been presented as a concern for automotive safety with a recommendation to perform sex-specific assessments (Yoganandan et al., 2017). Additionally, cervical vertebral body size and shape differences have been related to sex differences in the rates of injury (Stemper et al., 2008, Parenteau et al., 2014, Seacrist et al., 2012, Yoganandan et al., 2017), such as higher rates of vertebral fractures and mechanical stress in females due to the smaller size (Gilsanz et al., 1994). Further, sex differences in rate of sleep apnea have been related to neck circumference (Dancey et al., 2003), suggesting there could be a correlation between cervical vertebral body depth and the morphology of the vocal tract.

This study quantified growth from birth to 20 years, documenting the emergence of significant sexual dimorphism in both size and shape during the post-pubertal stage (cohort IV). These results highlight a limitation in the descriptions of CVMI stages, as they are not sex-specific and therefore homogenize the divergent shapes of adult males and females (Caldas et al., 2007). In fact, CVMI stages 5 and 6, the cohort IV equivalent stages, are often used to identify treatment timing (Baccetti et al., 2005); however, our findings show that this is the period when significant sex differences appear (Figure 3 and 4). Furthermore, the similarity of shape in females during cohort III and IV (Figure 3) with continued growth in cohort IV for size (Figure 1, center panel) and form (Figure 4) suggest shape alone is only one element to consider in maturation. Moreover, the sexual dimorphism of shape and size found in this study could explain the reported poor reliability of rater interpretation and identification of the final maturation stage of CVMI (Gray et al., 2016, Nestman et al., 2011, Santiago et al., 2012).

Future directions

The current practice of landmark-based methodology, refined in this study with the pre-process step, provides insight into the growth in size, shape, and form of the cervical vertebral bodies. However, the landmark-based 2D wireframes could be further enhanced by refining the boundaries of each cervical vertebral body for detailed analysis of shape and form, allowing additional insight into the functional impact on morphological development. Also, while the inclusion of both full and partial GPA in the morphometric analysis of this study allowed discourse regarding both shape and form, in-depth statistical analysis—such as ontogenetic trajectories and/or principal component analysis (PCA) of the Procrustes shape coordinates in combination with linear superioinferior height or anteroposterior depth measures—would provide further insight on morphological changes of cervical vertebral bodies. Furthermore, this study focused on the 2D wireframe to compare with the current clinical practice of assessing skeletal maturation in the midsagittal plane, however the morphological development of the 3D shape would provide greater information on sexual dimorphism and the inter-relationships between form and function.

Conclusions

While all human cervical vertebral bodies grow in size and shape during the first two decades of life, C2 obtains most of its adult size in early childhood, making the growth trend and rate of C2 distinct from C3-C7. While we had expected the growth of all cervical vertebral bodies to be similar, the C2 growth difference could be related to its distinct ossification pattern, connection and proximity to the skull, and the additional functional demands of head rotation placed on C2. Another important finding is that sexual dimorphism is present in the size, form, and shape of the cervical bodies. Regarding size, females have larger vertebrae up to age five, however, by the end of puberty, growth in males outpaces females and continues for a longer duration. Sexual dimorphism of cervical vertebral bodies form and shape becomes more distinct due to females reaching their adult shape earlier and male cervical vertebral bodies gaining additional anteroposterior growth in depth after about age 15 years. The strong evidence for sexual dimorphism in size, form, and shape suggest sex-specific considerations would benefit all fields that assess cervical spine development and that further research is needed into the growth and development of male and female cervical vertebrae.

Acknowledgements

This research was funded, in part, by National Institutes of Health Grant R01 DC6282 from the National Institute on Deafness and Other Communicative Disorders (NIDCD), and Core Grants P30 HD03352 and U54 HD090256 from the National Institute of Child Health and Human Development (NICHD). There was no involvement of the funding sources in the research design, data collection, analysis, interpretation, writing of this paper, or the submission for publication. All authors declare there was no conflict of interest in the research reported in this study/paper.

We thank Ellie Fischer and Anna Buchholz for assistance in landmark placement, and Moo K. Chung for statistical consultation. We also thank Drs. Edward Bursu, Jacqueline Houtman, and four anonymous reviewers for their comments on earlier versions of this paper that greatly enhanced the accuracy and clarity of this paper.

Author Contributions

HKV and MMC conceived and designed the research approach. CAM and SJH developed the pre-processing step to calculate the measurements and conducted all data analyses. CAM and HKV drafted the manuscript after intensive discussion on findings and implications of findings with MMC. All the authors critically reviewed the final version of the manuscript and consented to this submission.

References

ADAMS, D. C., OTÁROLA-CASTILLO, E. & PARADIS, E. 2013. geomorph: anrpackage for the collection and analysis of geometric morphometric shape data. *Methods in Ecology and Evolution,* 4(4), 393-399.

AIELLO, L. & DEAN, C. 1990. *An Introduction to Human Evolutionary Anatomy,* Academic Press.

AKOBO, S., RIZK, E., LOUKAS, M., CHAPMAN, J. R., OSKOUIAN, R. J. & TUBBS, R. S. 2015. The odontoid process: a comprehensive review of its anatomy, embryology, and variations. *Childs Nervous System,* 31(11), 2025-2034.

ALTAN, M., NEBIOĞLU DALCı, Ö. & İŞERI, H. 2011. Growth of the cervical vertebrae in girls from 8 to 17 years. A longitudinal study. *The European Journal of Orthodontics,* 34(3), 327-334.

Analyze 12.0 [computer program], Overland Park, KS, AnalyzeDirect

ARLEGI, M., GOMEZ-OLIVENCIA, A., ALBESSARD, L., MARTINEZ, I., BALZEAU, A., ARSUAGA, J. L. & BEEN, E. 2017. The role of allometry and posture in the evolution of the hominin subaxial cervical spine. *J Hum Evol,* 104(80-99.

ASHBURNER, J. & FRISTON, K. J. 2000. Voxel-based morphometry--the methods. *Neuroimage,* 11(6 Pt 1), 805-21.

BACCETTI, T., FRANCHI, L. & MCNAMARA, J. A. 2005. The cervical vertebral maturation (CVM) method for the assessment of optimal treatment timing in dentofacial orthopedics. *Seminars in Orthodontics,* 11(3), 119-129.

BEEN, E., SHEFI, S. & SOUDACK, M. 2017. Cervical lordosis: the effect of age and gender. *Spine J,* 17(6), 880-888.

BENCH, R. W. 1963. Growth of the cervical vertebrae as related to tongue, face, and denture behavior. *American Journal of Orthodontics,* 49(3), 183-214.

BICK, E. M. & COPEL, J. W. 1950. Longitudinal growth of the human vertebra: A contribution to human ostegeny. *Journal of Bone and Joint Surgery,* 32(4), 803-814.

BLAND, J. M. & ALTMAN, D. G. 1995. Multiple significance tests: the Bonferroni method. *BMJ,* 310(6973), 170.

BOË, L.-J., GRANAT, J., BADIN, P., AUTESSERRE, D., POCHIC, D., ZGA, N., HENRICH, N. & MÉNARD, L. 2006. Skull and vocal tract growth from newborn to adult. *In 7th International Seminar on Speech Production, ISSP7 (pp. 75-82).* UFMG, Belo Horizonte, Brazil.

BOGDUK, N. & MERCER, S. 2000. Biomechanics of the cervical spine. I: Normal kinematics. *Clinical Biomechanics,* 15(9), 633-648.

BYRD, S. E. & COMISKEY, E. M. 2007. Postnatal maturation and radiology of the growing spine. *Neurosurgery Clinics of North America,* 18(3), 431-61.

CALDAS, M. D. P., AMBROSANO, G. M. B. & HAITER-NETO, F. 2007. Use of cervical vertebral dimensions for assessment of children growth. *Journal of applied oral science,* 15(2), 144-147.

CARINHENA, G., SIQUEIRA, D. F. & SANNOMIYA, E. K. 2014. Skeletal maturation in individuals with Down's syndrome: comparison between PGS curve, cervical vertebrae and bones of the hand and wrist. *Dental press journal of orthodontics,* 19(4), 58-65.

CDC. 2000. *National center for health statistics clinical growth charts for the United States* [Online]. Center for Disease Control and Prevention Available: http://www.cdc.gov/growthcharts/ [Accessed 2017].

CHATZIGIANNI, A. & HALAZONETIS, D. J. 2009. Geometric morphometric evaluation of cervical vertebrae shape and its relationship to skeletal maturation. *American Journal of Orthodontics and Dentofacial Orthopedics,* 136(4), 481-e1.

CLAUDE, J. 2008. *Morphometrics with R,* Springer New York.

DANCEY, D. R., HANLY, P. J., SOONG, C., LEE, B., SHEPARD, J. & HOFFSTEIN, V. 2003. Gender differences in sleep apnea: The role of neck circumference. *Chest journal,* 123(5), 1544-1550.

DE BOOR, C. 1978. *A practical guide to splines,* New York : Springer-Verlag, [1978] ©1978.

DOS SANTOS, M. F., DE LIMA, R. L., DE-ARY-PIRES, B., PIRES-NETO, M. A. & DE ARY-PIRES, R. 2010. Developmental steps of the human cervical spine: parameters for evaluation of skeletal maturation stages. *Anatomical science international,* 85(2), 105-14.

DRYDEN, I. L. & MARDIA, K. V. 2016. *Statistical Shape Analysis: with Applications in R*, John Whiley & Sons Ltd.

EZRA, D., MASHARAWI, Y., SALAME, K., SLON, V., ALPEROVITCH-NAJENSON, D. & HERSHKOVITZ, I. 2017. Demographic aspects in cervical vertebral bodies' size and shape (C3-C7): a skeletal study. *The Spine Journal,* 17(1), 135-142.

FISHER, E., AUSTIN, D., WERNER, H. M., CHUANG, Y. J., BERSU, E. & VORPERIAN, H. K. 2016. Hyoid bone fusion and bone density across the lifespan: prediction of age and sex. *Forensic science, medicine, and pathology*.

FRANCIS, C. C. 1955. Dimensions of the cervical vertebrae. *The Anatomical Record,* 122(4), 603-609.

GILSANZ, V., BOECHAT, M. I., GILSANZ, R., LORO, M. L., ROE, T. F. & GOODMAN, W. G. 1994. Gender differences in vertebral sizes in adults: biomechanical implications. *Radiology,* 190(3), 678-682.

GILSANZ, V., KOVANLIKAYA, A., COSTIN, G., ROE, T., SAYRE, J. & KAUFMAN, F. 1997. Differential effect of gender on the sizes of the bones in the axial and appendicular skeletons. *The Journal of Clinical Endocrinology & Metabolism,* 82(5), 1603-1607.

GRAY, S., BENNANI, H., KIESER, J. A. & FARELLA, M. 2016. Morphometric analysis of cervical vertebrae in relation to mandibular growth. *American Journal of Orthodontics and Dentofacial Orthopedics,* 149(1), 92-98.

HASSEL, B. & FARMAN, A. G. 1995. Skeletal maturation evaluation using cervical vertebrae. *American Journal of Orthodontics and Dentofacial Orthopedics,* 107(1), 58-66.

HELLSING, E. 1991. Cervical vertebral dimensions in 8- 11- and 15-year-old children. *Acta odontologica Scandinavica,* 49(4), 207-213.

HUELKE, D. F. An overview of anatomical considerations of infants and children in the adult world of automobile safety design. In Annual Proceedings / Association for the Advancement of Automotive Medicine (Vol. 42), 1998. Association for the Advancement of Automotive Medicine, 93-113.

JAQUEIRA, L. M., ARMOND, M. C., PEREIRA, L. J., ALCANTARA, C. E. & MARQUES, L. S. 2010. Determining skeletal maturation stage using cervical vertebrae: evaluation of three diagnostic methods. *Braz Oral Res,* 24(4), 433-7.

JOHNSON, K. T., AL-HOLOU, W. N., ANDERSON, R. C., WILSON, T. J., KARNATI, T., IBRAHIM, M., GARTON, H. J. & MAHER, C. O. 2016. Morphometric analysis of the developing pediatric cervical spine. *Journal of Neurosurgery: Pediatrics,* 18(3), 377-389.

KASAI, T., IKATA, T., KATOH, S., MIYAKE, R. & TSUBO, M. 1996. Growth of the cervical spine with special reference to its lordosis and mobility. *Spine* 21(18), 2067-2073.

KELLY, M. P., VORPERIAN, H. K., WANG, Y., TILLMAN, K. K., WERNER, H. M., CHUNG, M. K. & GENTRY, L. R. 2017. Characterizing mandibular growth using three-dimensional imaging techniques and anatomic landmarks. *Arch Oral Biol,* 77(27-38.

KLINGENBERG, C. P. 2016. Size, shape, and form: concepts of allometry in geometric morphometrics. *Dev Genes Evol,* 226(3), 113-37.

KOKOSKA, E. R., KELLER, M. S., RALLO, M. C. & WEBER, T. R. 2001. Characteristics of pediatric cervical spine injuries. *Journal of pediatric surgery,* 36(1), 100-105.

KUMARESAN, S., YOGANANDAN, N., PINTAR, F. A., MAIMAN, D. J. & KUPPA, S. 2000. Biomechanical study of pediatric human cervical spine: a finite element approach. *Journal of Biomechanical Engineering,* 122(1), 60-71.

LE HUEC, J. C., SADDIKI, R., FRANKE, J., RIGAL, J. & AUNOBLE, S. 2011. Equilibrium of the human body and the gravity line: the basics. *European Spine Journal,* 20(5), 558-563.

LIEBERMAN, D. E. 2007. The evolution of human speech: Its anatomical and neural bases. *Current Anthropology,* 48(1), 39-66.

LIEBERMAN, D. E., MCCARTHY, R. C., HIIEMAE, K. M. & PALMER, J. B. 2001. Ontogeny of postnatal hyoid and larynx descent in humans. *Archives of Oral Biology,* 46(2)**,** 117-128.

LOURYAN, S., VANMUYLDER, N. & BRUNEAU, M. 2011. Embryology of the cervical spine and cranio-vertebral junction. *Pathology and surgery around the vertebral artery.* Paris: Springer Paris.

LUSTRIN, E. S., KARAKAS, S. P., ORTIZ, A. O., CINNAMON, J., CASTILLO, M. & VALIATHAN, M. 2003. Pediatric cervical spine: normal anatomy, variants, and trauma. *Radiographics,* 23(3)**,** 539-560.

MASON, K. N., PERRY, J. L., RISKI, J. E. & FANG, X. 2016. Age related changes between the level of velopharyngeal closure and the cervical spine. *The Journal of craniofacial surgery,* 27(2)**,** 498-503.

MENEZES, A. H. & TRAYNELIS, V. C. 2008. Anatomy and biomechanics of normal craniovertebral junction (a) and biomechanics of stabilization (b). *Child's Nervous System,* 24(10)**,** 1091-1100.

MITTEROECKER, P., GUNZ, P., WINDHAGER, S. & SCHAEFER, K. 2013. A brief review of shape, form, and allometry in geometric morphometrics, with applications to human facial morphology. *Hystrix, the Italian Journal of Mammalogy*.

NALLEY, T. K. & GRIDER-POTTER, N. 2015. Functional morphology of the primate head and neck. *American journal of physical anthropology,* 156(4)**,** 531-542.

NELLHAUS, G. 1968. Head circumference from birth to eighteen years. Practical composite international and interracial graphs. *Pediatrics,* 41(1)**,** 106-14.

NESTMAN, T. S., MARSHALL, S. D., QIAN, F., HOLTON, N., FRANCISCUS, R. G. & SOUTHARD, T. E. 2011. Cervical vertebrae maturation method morphologic criteria: poor reproducibility. *American Journal of Orthodontics and Dentofacial Orthopedics,* 140(2)**,** 182-188.

NITECKI, S. & MOIR, C. R. 1994. Predictive factors of the outcome of traumatic cervical spine fracture in children. *Journal of Pediatric Surgery,* 29(11)**,** 1409-1411.

PANG, D. & THOMPSON, D. N. 2011. Embryology and bony malformations of the craniovertebral junction. *Child's Nervous System,* 27(4)**,** 523-64.

PARENTEAU, C. S., WANG, N. C., ZHANG, P., CAIRD, M. S. & WANG, S. C. 2014. Quantification of pediatric and adult cervical vertebra-anatomical characteristics by age and gender for automotive application. *Traffic Injury Prevention,* 15(6)**,** 572-582.

PIATT, J. H., JR. & GRISSOM, L. E. 2011. Developmental anatomy of the atlas and axis in childhood by computed tomography. *Journal of Neurosurgery: Pediatrics,* 8(3)**,** 235-243.

PICHAI, S., RAJESH, M., REDDY, N., ADUSUMILLI, G., REDDY, J. & JOSHI, B. 2014. A comparison of hand wrist bone analysis with two different cervical vertebral analysis in measuring skeletal maturation. *Journal of International Oral Health,* 6(5)**,** 36-41.

SAN ROMÁN, P., PALMA, J. C., OTEO, M. D. & NEVADO, E. 2002. Skeletal maturation determined by cervical vertebrae development. *The European Journal of Orthodontics,* 24(3)**,** 303-311.

SANTIAGO, R. C., DE MIRANDA COSTA, L. F., VITRAL, R. W., FRAGA, M. R., BOLOGNESE, A. M. & MAIA, L. C. 2012. Cervical vertebral maturation as a biologic indicator of skeletal maturity. *The Angle orthodontist,* 82(6)**,** 1123-1131.

SCAMMON, R. E. 1930. The Measurement of the Body in Childhood. *In:* HARRIS, J. A., JACKSON, C. M., PATTERSON, D. G. & SCAMMON, R. E. (eds.) *The Measurement of Man.* Minneapolis: University of Minnesota Press.

SEACRIST, T., SAFFIOTI, J., BALASUBRAMANIAN, S., KADLOWEC, J., STERNER, R., GARCIA-ESPANA, J. F., ARBOGAST, K. B. & MALTESE, M. R. 2012. Passive cervical spine flexion: The effect of age and gender. *Clinical Biomechanics,* 27(4)**,** 326-333.

SHAPLAND, F. & LEWIS, M. E. 2014. Brief communication: a proposed method for the assessment of pubertal stage in human skeletal remains using cervical vertebrae maturation. *American journal of physical anthropology,* 153(1)**,** 144-153.

STEMPER, B. D., YOGANANDAN, N., PINTAR, F. A., MAIMAN, D. J., MEYER, M. A., DEROSIA, J., SHENDER, B. S. & PASKOFF, G. 2008. Anatomical gender differences in cervical vertebrae of size-matched volunteers. *Spine,* 33(2)**,** E44-E49.
TULSI, R. S. 1971. Growth of the human vertebral column. An osteological study. *Cells Tissues Organs,* 79(4)**,** 570-580.
VORPERIAN, H. K., WANG, S., CHUNG, M. K., SCHIMEK, E. M., DURTSCHI, R. B., KENT, R. D., ZIEGERT, A. J. & GENTRY, L. R. 2009. Anatomic development of the oral and pharyngeal portions of the vocal tract: an imaging study. *Journal of the Acoustical Society of America,* 125(3)**,** 1666-1678.
WANG, J. C., NUCCION, S. L., FEIGHAN, J. E., COHEN, B., DOREY, F. J. & SCOLES, P. V. 2001. Growth and development of the pediatric cervical spine documented radiographically. *Journal of Bone and Joint Surgery,* 83(8)**,** 1212-1218.
WANG, Y., CHUNG, M. K. & VORPERIAN, H. K. 2013. Composite growth model applied to human oral and pharyngeal structures and identifying the contribution of growth types. *Statistical Methods in Medical Research,* 25(5)**,** 1975-1990.
WHO. 2006. *Multicentre Growth Reference Study Group. WHO Child Growth Standards: Length/height-for-age, weight-for-age, weight-for-length, weight-for-height and body mass index-for-age: Methods and development* [Online]. Geneva: World Health Organization. Available: http://www.who.int/childgrowth/en/ [Accessed 2017].
YANG, Y. M., LEE, J., KIM, Y. I., CHO, B. H. & PARK, S. B. 2014. Axial cervical vertebrae-based multivariate regression model for the estimation of skeletal-maturation status. *Orthodontics & craniofacial research,* 17(3)**,** 187-196.
YOGANANDAN, N., BASS, C. R., VOO, L. & PINTAR, F. A. 2017. Male and female cervical spine biomechanics and anatomy: Implication for scaling injury criteria. *Journal of Biomechanical Engineering,* 139(5)**,** 054502-1 - 054502-5.
YOGANANDAN, N., PINTAR, F. A., LEW, S. M., RAO, R. D. & RANGARAJAN, N. 2011. Quantitative analyses of pediatric cervical spine ossification patterns using computed tomography. *Annals of Advances in Automotive Medicine - 55th AAAM Annual Conference,* 55(October)**,** 159 - 168.
ZELDITCH, M. L., SWIDERSKI, D. L., SHEETS, H. D. & FINK, W. 2004. *Geometric morphometrics for Biologists: A primer,* Elsevier.

Tables

Table 1: Percent growth type, somatic or neural, in size/area for each of the cervical vertebral body for males and females. Findings indicate C2 growth type to be distinctly different from growth in C3-C7 where growth type is predominantly somatic. C2 growth type, however, is predominantly neural particularly in females.

Percent contribution of Somatic and Neural (%)				
	Male		**Female**	
	Somatic	**Neural**	**Somatic**	**Neural**
C2	39.64	60.36	8.78	91.22
C3	99.17	0.83	100.00	0.00
C4	99.25	0.75	98.77	1.23
C5	99.86	0.14	99.32	0.68
C6	99.93	0.07	98.77	1.23
C7	99.73	0.27	99.41	0.59

Table 2: Sexual dimorphism assessment in LDBM measures. Table lists the p-values from the t-tests/Mann-Whitney U tests on each age cohort between male and female. The landmark are labeled: apex, superior point of C2; ai, anterior inferior; pi, posterior inferior; ps, posterior superior; as, anterior superior with numbers referencing the cervical vertebrae C2-C7. Age cohorts with significant sex differences, as identified with Bonferroni corrected $\alpha = 0.05$ significance level of 0.008, are denoted with an asterisk (*).

	p-value of LDBM			
	Cohort I	**Cohort II**	**Cohort III**	**Cohort IV**
Apex	0.1668	0.9887	0.5224	0.0762
C2ai	0.2887	0.5638	0.7663	0.1396
C2pi	0.0557	0.5119	0.5101	0.0001 *
C3as	0.5798	0.9051	0.0773	0.0078 *
C3ai	0.1349	0.8518	0.1375	0.4956
C3pi	0.3382	0.8348	0.2531	0.0000 *
C3ps	0.2586	0.7269	0.2042	0.0018 *
C4as	0.1463	0.8877	0.1153	0.0001 *
C4ai	0.0411	0.9192	0.4374	0.0080 *
C4pi	0.2642	0.8691	0.0329	0.0014 *
C4ps	0.1720	0.9458	0.1411	0.0052 *
C5as	0.2925	0.9546	0.0340	0.0001 *
C5ai	0.0847	0.7172	0.6166	0.0020 *
C5pi	0.1973	0.4813	0.1628	0.0020 *
C5ps	0.1257	0.9546	0.1787	0.0015 *

C6as	0.6363	0.9487	0.1072	0.0003 *
C6ai	0.2817	0.6305	0.5479	0.0002 *
C6pi	0.1640	0.9144	0.0174	0.0004 *
C6ps	0.3523	0.8534	0.2289	0.0692
C7as	0.0943	0.9748	0.1902	0.0025 *
C7ai	0.4630	0.5288	0.4858	0.0510
C7pi	0.0395	0.8324	0.2207	0.0000 *
C7ps	0.2960	0.5205	0.6937	0.0000 *

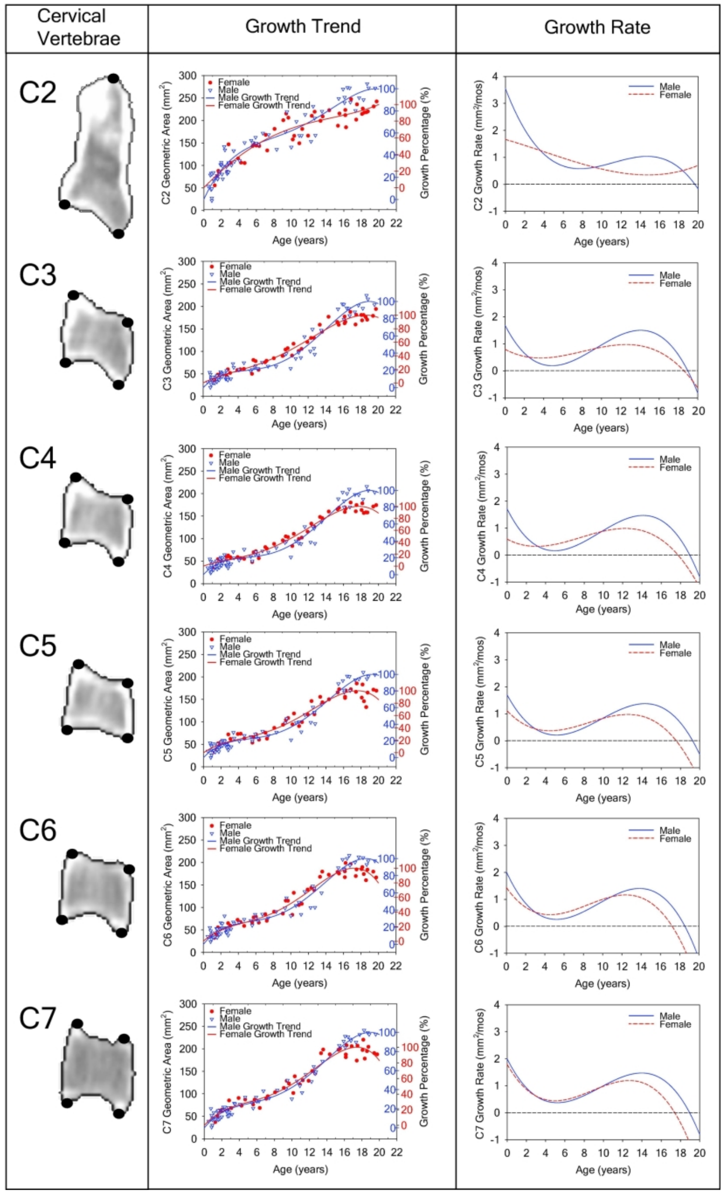

Left Panel: Exhibits the anatomical placement of the 23 landmarks on each cervical vertebral body in the midsagittal plane as visualized on the CT of an adult female at 17 years and 1 month (subject F220). Each landmark is placed at the margins of the vertebral body. The orientation of the cervical vertebral bodies is as follows: the left side is the posterior border, the right is the anterior border, the top is the superior border, and the bottom is the inferior border. Center Panel: Geometric areas for males (open triangle) and females (fill circles) plotted as a function of age, with sex-specific fourth degree polynomial fits representing the growth trend for each cervical vertebra. Each plot has a second y-axis denoting the male (inner) and female (outer) percent of adult growth. Right Panel: The first derivative of the sex-specific growth trends are plotted for each cervical vertebra to represent the growth rate. The growth rate is plotted in millimeters by month (mm^2/mos).

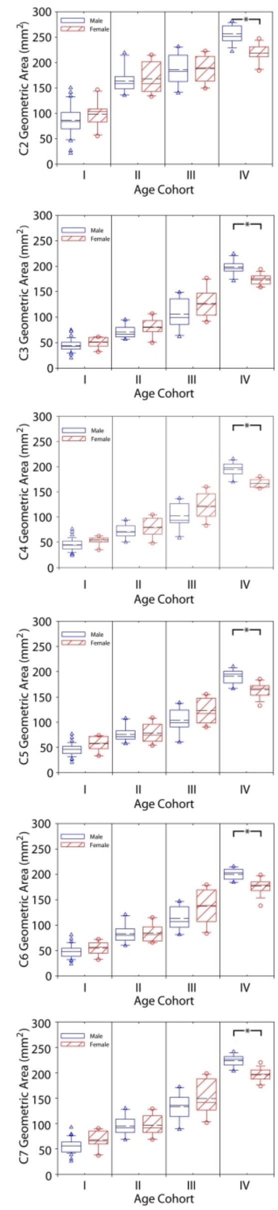

Boxplots of each cervical vertebral body geometric area for males (blue) and female (red) at four discrete age cohorts (cohort I, ages birth to 4:11 (years: months); cohort II, ages 5:00 to 9:11; cohort III, ages 10:00 to 14:11; and cohort IV, ages 15:00 to 19:11). The upper and lower bounds of each box presents the 75th and 25th percentiles respectively, with the mean (solid line), and median (dashed line) per age cohort. Significant sex differences for age cohort are denoted with an asterisk (*).

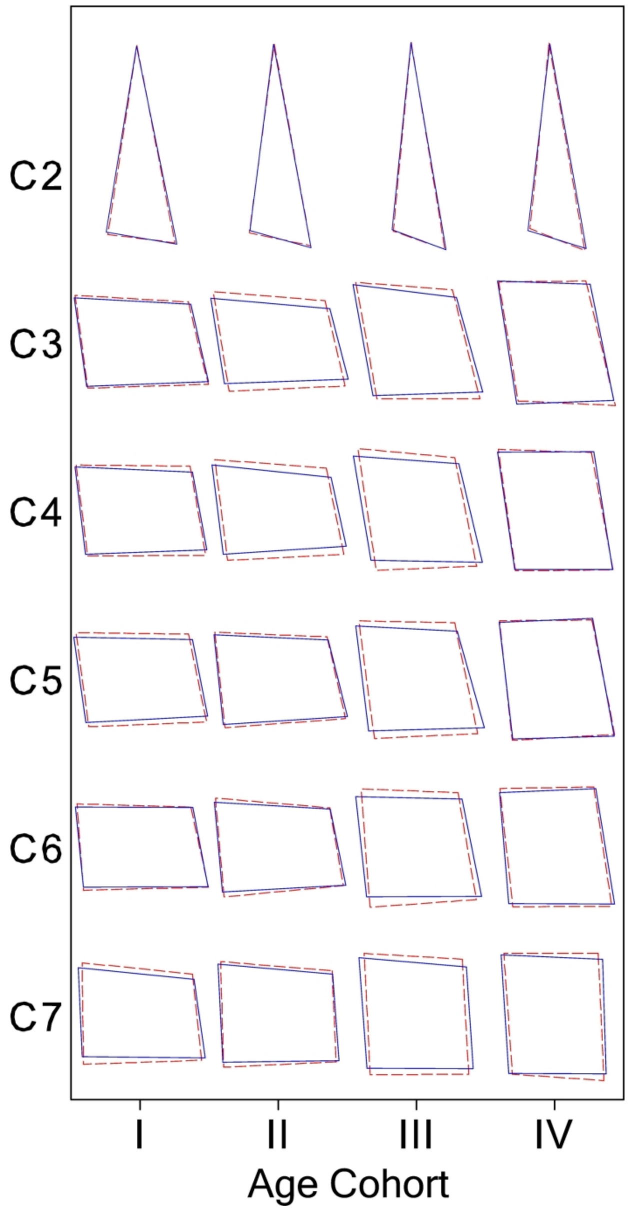

Visualization of the morphologic changes of the mean vertebral body wireframes in males and females across the four age cohorts, using full General Procrustes Analysis, with the posterior edge on the left and the anterior edge on the right. For C3-C7, note the transition in average shape across the four age cohorts, from small horizontal rectangle to, wedge shape, to square and finally to vertical rectangle. The average male (blue) and female (red-dashed) mean shapes are plotted by age cohort for each cervical vertebral body. The vertebral wireframe orientation is described in the Figure 1 legend.

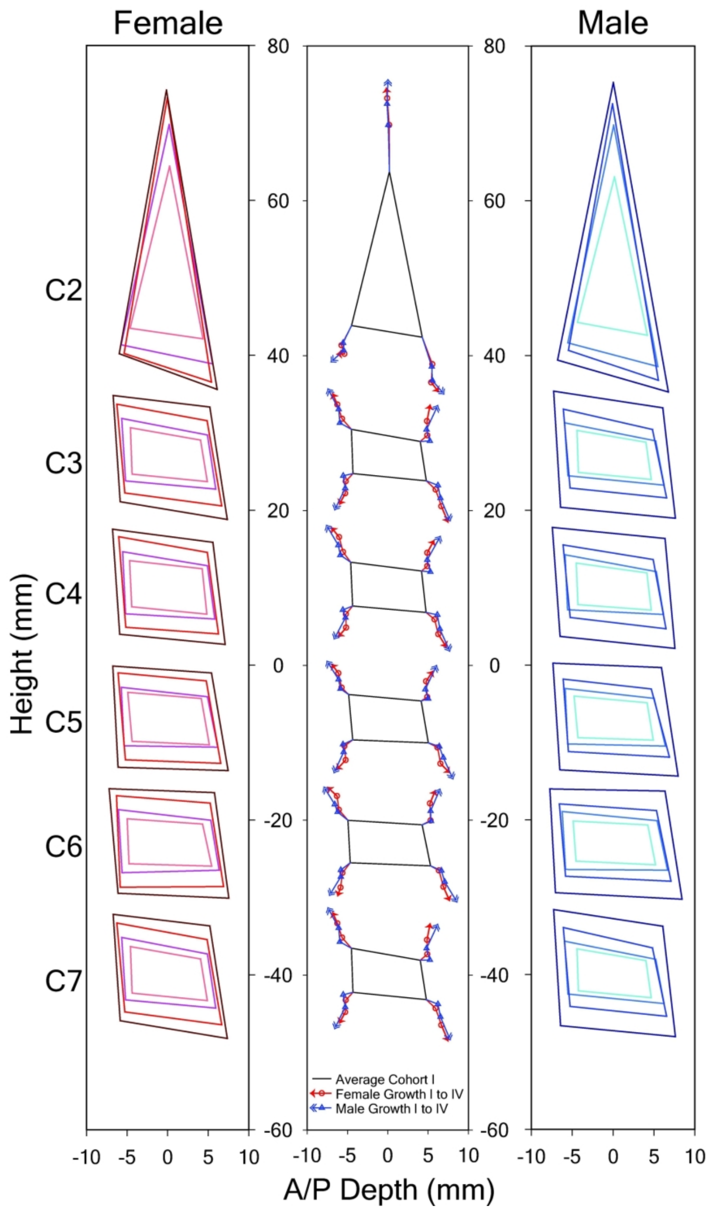

Superimposition of the mean vertebral wireframes of the four age cohorts for each vertebral body for females (left panel) and males (right panel). The center panel is a schematic of the male-female difference in the amount and direction of growth occurring at each landmark from age cohort I to cohort IV. The lines with double open arrows and triangles represent males, while the lines with a single filled arrow and circles represent females. The triangles and circles denote the mean landmark for males and females respectively at age cohort II then cohort III. The vertebral wireframe orientation is described in the Figure 1 legend.